

Laryngeal muscular control of vocal fold posturing: Numerical modeling and experimental validation

Jun Yin^{a)}

The State Key Lab of Fluid Power Transmission and Control Systems,
School of Mechanical Engineering, Zhejiang University, Hangzhou 310028, China
junyin@zju.edu.cn

Zhaoyan Zhang

UCLA School of Medicine, 31-24 Rehab Center, 1000 Veteran Avenue, Los Angeles,
California 90095-1794, USA
zyzhang@ucla.edu

Abstract: A three-dimensional continuum model of vocal fold posturing was developed to investigate laryngeal muscular control of vocal fold geometry, stiffness, and tension, which are difficult to measure in live humans or *in vivo* models. This model was able to qualitatively reproduce *in vivo* experimental observations of laryngeal control of vocal fold posturing, despite the many simplifications which are necessary due to the lack of accurate data of laryngeal geometry and material properties. The results present a first comprehensive study of the co-variations between glottal width, vocal fold length, stiffness, tension at different conditions of individual, and combined laryngeal muscle activation.

© 2016 Acoustical Society of America

[DDOS]

Date Received: January 11, 2016 **Date Accepted:** July 28, 2016

1. Introduction

Voice control is primarily achieved through intrinsic laryngeal muscle activation, which postures the vocal folds into desired geometry, stiffness, and tension conditions. Understanding this vocal fold posturing process is important for understanding voice control and the development of computational models of phonation. Clinically, such an understanding is essential for phonosurgery, the goal of which is to restore normal vocal fold posturing. Although the effects of intrinsic laryngeal muscle activation on vocal fold geometry have been investigated in experiment,¹⁻⁴ these studies were limited to an endoscopic superior view, and unable to provide information on the three-dimensional (3D) deformation of the vocal folds. More importantly, due to the lack of reliable *in vivo* measurement techniques, the stiffness and tension within the vocal folds were often not measured in these experimental studies. As a result, the effects of laryngeal muscle activation on vocal fold stiffness and tension, which play an important role in determining the resulting voice production,⁵ still remain unclear and speculative.⁶

Due to these experimental limitations, numerical models have been developed and used to investigate the physics of vocal fold posturing.^{5,7-10} In particular, models based on continuum mechanics^{5,8,9} allow physically-based, instead of rule-based, calculation of vocal fold deformation under laryngeal muscle activation, and thus have the potential to provide insight into the muscular control of the 3D deformation, stiffness, and tension within the vocal folds. Due to the complexity of the physics involved in laryngeal muscle activation and the lack of accurate data on the geometry and material properties of the vocal folds, laryngeal muscles, and laryngeal cartilages, simplifications were often made in these models to make the problem tractable. Thus, one may question that with the many simplifications, whether these continuum models are still able to at least qualitatively reproduce the realistic vocal fold posturing and provide useful insight into our understanding of vocal fold posturing. Indeed, model validation by comparison to experiment is seldom attempted in previous studies.

This paper presents a comprehensive numerical model of vocal fold posturing, including all intrinsic laryngeal muscles [the thyroarytenoid (TA), cricothyroid (CT),

^{a)} Author to whom correspondence should be addressed. Also at: Key Laboratory of 3D Printing Process and Equipment of Zhejiang Province's, School of Mechanical Engineering, Zhejiang University, Hangzhou 310028, China.

lateral cricoarytenoid (LCA), interarytenoid (IA), and the posterior cricoarytenoid (PCA) muscles], and three relevant cartilages (thyroid, cricoid, and arytenoid). The goal was to investigate (1) whether the model is able to qualitatively reproduce observations from *in vivo* larynx experiments, and (2) the co-variations of the glottal gap, vocal fold length, stiffness, tension, and eigenfrequencies at different conditions of individual and combined laryngeal muscle activation.

2. Numerical model

2.1 Geometry and boundary conditions

The geometry of cricoid and arytenoid cartilages was obtained from the magnetic resonance images of human laryngeal cartilages by Selbie *et al.*,¹¹ which was converted into a computer solid model by Hunter and Thomson,¹² while a simplified geometry was used for the thyroid cartilage [Figs. 1(B) and 1(C)]. Due to the lack of information to separate the different layers within the vocal folds, a body-cover two-layer simplified vocal fold model^{13,14} was used in this study [Fig. 1(D)]. Due to the lack of detailed geometric data, all laryngeal muscles except TA were simplified as cylinders with different cross section areas [Figs. 1(B) and 1(C)], and the origin and insertion points of laryngeal muscles were estimated based on experimental observation.¹⁰ Note that the CT muscle included two bundles, the vertical part (CTv) and the oblique part (CTo). Because the transverse and oblique IA muscles have a similar effect of transversely approximating the arytenoid cartilages,¹⁵ these two IA bundles were merged and modeled as one muscle bundle in this study. The interaction of arytenoid and the cricoid cartilages within the cricoarytenoid joint was assumed to be a “contact-sliding” interface as described by Yin and Zhang,⁹ while the thyroid cartilage at the cricothyroid joint was allowed a rigid rotation motion around the *z* axis and a forward-backward gliding movement [Fig. 1(B)].

2.2 Constitutive models

Because the cartilages are much stiffer than the vocal folds and muscles and are expected to exhibit small deformations, they were simulated in this study as a nearly incompressible linear elastic material with a Young’s modulus of 100 MPa and a Poisson’s ratio of 0.47, similar to previous studies.^{8–10} The vocal fold and laryngeal muscles were modeled as hyperelastic materials, with the corresponding strain energy density function (SEDF) consisting of both a passive ($W^{passive}$) and an active (W^{active}) component.⁹ The cover layer of the vocal fold has only a passive component, which is described by the nearly incompressible Yeoh model as

$$W^{passive} = c_1(\bar{I}_1 - 3) + c_2(\bar{I}_1 - 3)^2 + c_3(\bar{I}_1 - 3)^3 + \frac{\kappa}{2}(J - 1)^2, \tag{1}$$

where \bar{I}_1 is the modified first invariant, J is the volume ratio between the deformed and undeformed geometry, and κ is the initial bulk modulus. The material constants of the Yeoh model were determined by fitting the uniaxial stretch-stress data obtained from human vocal folds so that $c_1 = 1.23 \times 10^3$ Pa, $c_2 = 6.51 \times 10^3$ Pa, $c_3 = 3.07 \times 10^4$ Pa, and $\kappa = 3 \times 10^6$ Pa.¹⁶ The active component of SEDF was formulated similarly as in our previous work⁹

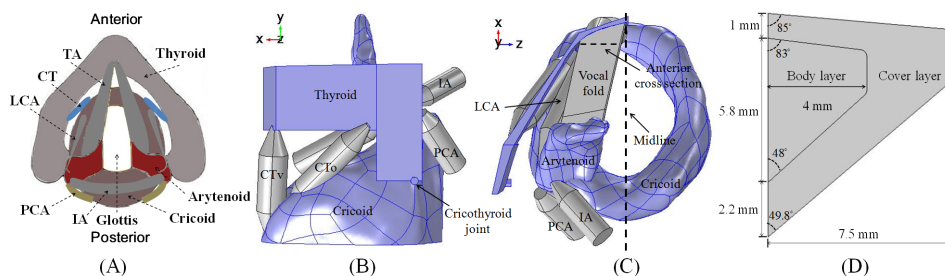


Fig. 1. (Color online) (A) A sketch of the laryngeal framework including the vocal fold, the thyroid, cricoid, and arytenoid cartilages, and the LCA, IA, PCA, and CT muscles from a superior view. (B) and (C) show the numerical model developed in this study from a side view and superior view, respectively. (D) The cross section dimensions of the vocal fold used in the model. Note that only the left vocal fold is shown in (C) because only one fold was modeled in this study due to imposed left–right symmetry.

$$W^{\text{active}} = \begin{cases} \frac{\alpha\sigma^{\text{max}}}{3} \left[4 \left(1 - \frac{\lambda}{\lambda_{\text{off}}} \right)^2 - 3 \right] \left(1 - \frac{\lambda}{\lambda_{\text{off}}} \right), & 0.5\lambda_{\text{off}} \leq \lambda \leq 1.4\lambda_{\text{off}} \\ 0, & \text{otherwise} \end{cases} \quad (2)$$

where α is the muscle activation level varying from 0 (at rest) to 1 (maximum activation), σ^{max} is the maximum active stress value, λ is the stretch along the muscle fiber direction, and $\lambda_{\text{off}}=1.4$ is the optimal stretch of muscle fiber at which σ^{max} occurs. The TA, LCA, and PCA muscles were assumed to have the same activation strength ($\sigma_{\text{TA}}^{\text{max}} = \sigma_{\text{LCA}}^{\text{max}} = \sigma_{\text{PCA}}^{\text{max}} = 1.05 \times 10^5 \text{ Pa}$);⁸ whereas the IA activation was set to be $\sigma_{\text{IA}}^{\text{max}} = 2\sigma_{\text{TA}}^{\text{max}}$, since the transverse and oblique IA muscles were merged into one muscle bundle. Experimentally, the oblique bundle of CT muscle was much stronger than the vertical one,¹ thus in this study $\sigma_{\text{CTo}}^{\text{max}} = 1.5\sigma_{\text{TA}}^{\text{max}}$, and $\sigma_{\text{CTv}}^{\text{max}} = 0.5\sigma_{\text{TA}}^{\text{max}}$.

The numerical model was developed using the commercial software COMSOL. For each muscle condition, a static simulation was used to determine vocal fold deformation, from which an estimation of vocal fold stiffness along the anterior-posterior (AP) direction was defined as Eq. (14) in a previous paper.⁵ A pre-stressed eigenmode analysis was then performed on the deformed vocal folds to investigate how laryngeal muscle activation affects vocal fold eigenfrequencies,^{5,9} which play an important role in the glottal fluid-structure interaction.¹⁷

3. Results

3.1 Model validation

Current *in vivo* experiments of vocal fold posturing are often limited to a superior observation of vocal fold vibration.^{2,3} In this study, model validation was achieved by comparing the glottal configuration from a superior view (the edge of the glottis when viewed from above) predicted by our model to the experimental observations under different conditions of individual and combined laryngeal muscle activation in Chhetri *et al.* (2012).³ As shown in Fig. 2, contraction of the TA muscle caused the vocal folds to move toward the glottal midline [Fig. 2(B)], particularly at the anterior portion, which led to complete glottal closure at the membranous (anterior) portion but left a gap at the posterior portion. Combined activation of the LCA and IA muscles closed the posterior portion of the glottis but left a gap in the anterior portion of the glottis [Fig. 2(C)]. Complete glottal closure at both the anterior and posterior portions was achieved with a combined activation of the LCA/IA/TA muscles [Fig. 2(D)]. The antagonistic role of the CT and TA muscles in controlling vocal fold elongation and the anterior glottal opening was also observed: CT activation elongated and slightly abducted the vocal folds [Fig. 2(E)] whereas the TA activation shortened and adducted the vocal folds [Fig. 2(F)]. The abduction effect of the CT muscle was also shown in Fig. 2(G). The animations of sequential activations of LCA/IA/TA and LCA/IA/CT muscles are displayed in Mm. 1. In general, our numerical model was able to qualitatively reproduce these experimental observations.

Mm. 1. Numerical modeling of LCA/IA/TA and LCA/IA/CT muscle activation. This is file type mp4 (1 Mb).

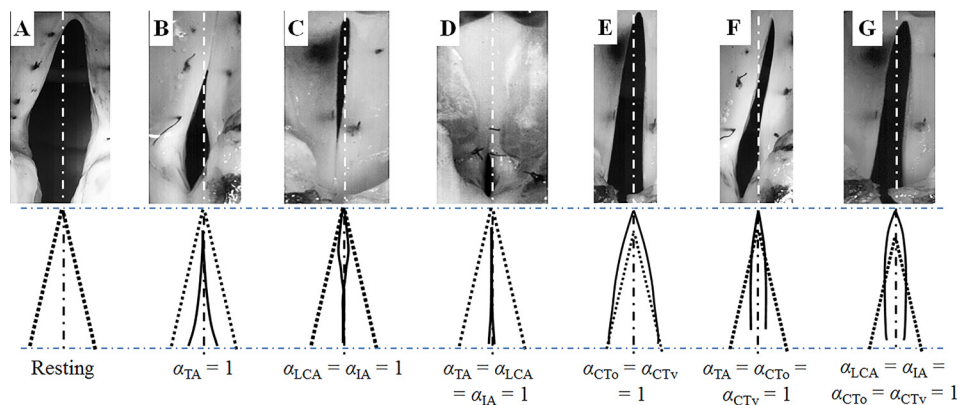


Fig. 2. (Color online) Top view of the glottal configuration at different muscular conditions. The images in the first row are experimental observations adapted from Chhetri *et al.* (2012) (Ref. 3). The dotted lines in the lower panel indicate the resting glottal configuration from a superior view.

3.2 Effect of laryngeal muscle activation

Figure 3 shows the effect of laryngeal muscle activation on vocal fold length, anterior and posterior glottal widths [Figs. 3(A) and 3(B)], vocal fold stiffness [Figs. 3(D) and 3(F)], and tension [Figs. 3(C) and 3(E)], and the first vocal fold *in vacuo* eigenfrequency [Fig. 3(G)]. Depending on the degree of vocal fold AP elongation, Fig. 3 can be divided into three regions: a vocal fold-elongating region (elongation > 0.1); a vocal fold-shortening region (elongation < -0.1); and a neutral region (-0.1 < elongation < 0.1). The effect of the vertical bundle of the CT muscle seemed to have a much smaller effect on vocal fold elongation than the oblique bundle. Generally, muscle conditions leading to vocal fold shortening also led to adduction of the anterior portion of the glottis, whereas vocal fold elongation led to abduction of the anterior glottis [Fig. 3(A)], indicating a dominant role of the TA/CT in the control of the anterior glottal opening. Control of the posterior glottal opening was more complex, with the LCA/IA/PCA also having important influence [Fig. 3(B)].

Because the vocal fold cover layer consisted of only passive soft tissues, AP stress in the cover layer was primarily dependent on the degree of vocal fold deformation, with positive stress (tension) at conditions of elongation and negative stress (compression) at conditions of vocal fold shortening [Fig. 3(C)]. The AP stiffness in the cover layer was minimum at the original undeformed state of the vocal fold, and increased with either elongation or shortening [Fig. 3(D)], similar to our previous observation.⁵ The AP stress in the body layer was minimum when the vocal folds were not much elongated and increased with either elongation or shortening of the vocal folds. Note that the highest AP stress in the body layer was obtained when both the TA and CT muscles were activated [Fig. 3(E)]. A similar pattern can be observed for the AP stiffness in the body [Fig. 3(F)].

The first eigenfrequency of the vocal fold under different muscular activation conditions [Fig. 3(G)] followed a pattern similar to those of the AP stiffness [Figs. 3(D) and 3(F)], increasing with either vocal fold elongation or shortening, and was primarily determined by the interaction between the TA and CTo muscles. The effects of other muscles appear to be almost negligible. It is worth noting that the highest first eigenfrequency was obtained when the CT muscle activation was accompanied by the activation of the PCA muscle [Fig. 3(G)]. The largest vocal fold elongation and highest AP stress and stiffness in the cover layer were also observed under simultaneous activation of CT

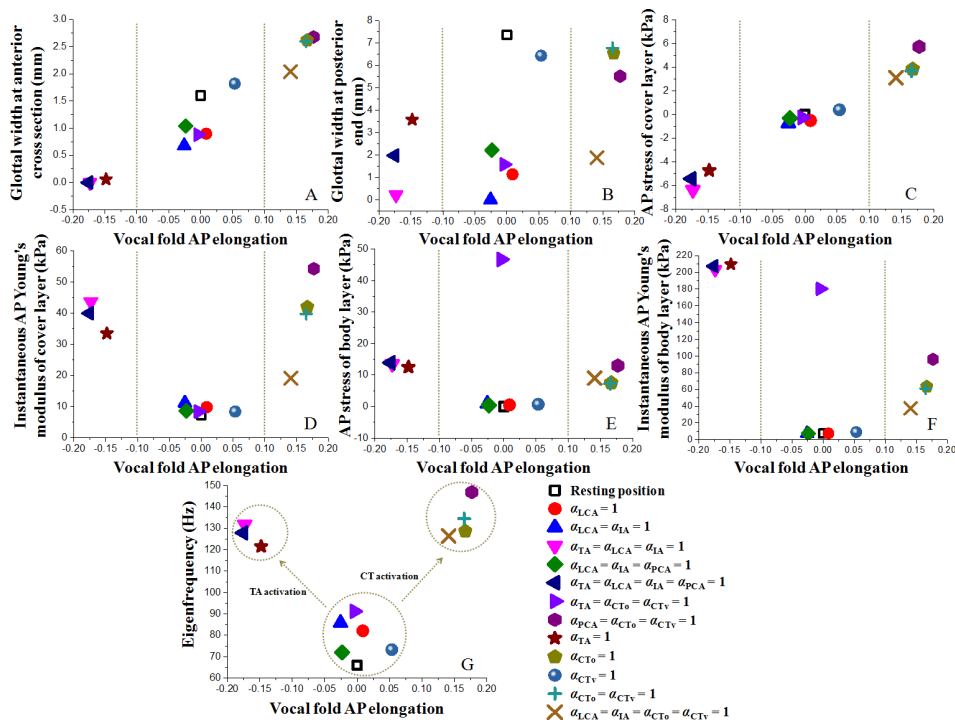


Fig. 3. (Color online) The relations between vocal fold AP elongation and (A) glottal width at anterior cross section [shown in Fig. 1(C)], (B) glottal width at posterior end, (C) average AP stress of cover layer, (D) instantaneous Young's modulus along AP direction of cover layer, (E) average AP stress of body layer, (F) instantaneous Young's modulus along AP direction of body layer, and (G) the first *in vacuo* vocal fold eigenfrequency.

and PCA muscles. This is probably because the vocal folds need to be pulled from both ends in order to achieve maximum elongation.

4. Conclusion

This study shows that our continuum model of vocal fold posturing agreed reasonably well with observations from *in vivo* larynx experiments, despite the many model simplifications which are necessary due to the lack of experimental data of laryngeal geometry and material properties. Our preliminary results present a first comprehensive study of the co-variations between glottal width, vocal fold length, stiffness, tension, and eigenfrequencies at different conditions of individual and combined laryngeal muscle activation. In the future, this vocal fold posturing model will be coupled with a glottal fluid-structure interaction model so that the effect of individual and combined laryngeal muscle activation on voice production can be predicted.

Acknowledgments

This study was supported by National Natural Science Foundation of China (NSFC) Grant No. 11402056, and NIH research Grant Nos. R01DC011299 and R01DC009229.

References and links

- ¹K. H. Hong, M. Ye, Y. M. Kim, K. F. Kevorkian, J. Kreiman, and G. S. Berke, "Functional differences between the two bellies of the cricothyroid muscle," *Otolaryngol. Head Neck Surg.* **118**(5), 714–722 (1998).
- ²H. Choi, M. Ye, and G. S. Berke, "Function of the interarytenoid (IA) muscle in phonation: In vivo laryngeal model," *Yonsei Med. J.* **36**(1), 58–67 (1995).
- ³D. K. Chhetri, J. Neubauer, and D. A. Berry, "Neuromuscular control of fundamental frequency and glottal posture at phonation onset," *J. Acoust. Soc. Am.* **131**(2), 1401–1412 (2012).
- ⁴D. K. Chhetri, J. Neubauer, E. Sofer, and D. A. Berry, "Influence and interactions of laryngeal adductors and cricothyroid muscles on fundamental frequency and glottal posture control," *J. Acoust. Soc. Am.* **135**, 2052–2064 (2014).
- ⁵J. Yin and Z. Zhang, "The influence of thyroarytenoid and cricothyroid muscle activation on vocal fold stiffness and eigenfrequencies," *J. Acoust. Soc. Am.* **133**(5), 2972–2983 (2013).
- ⁶M. Hirano, "Morphological structure of the vocal fold and its variations," *Folia Phoniatr.* **26**, 89–94 (1974).
- ⁷G. R. Farley, "A biomechanical laryngeal model of voice F_0 and glottal width control," *J. Acoust. Soc. Am.* **100**(6), 3794–3812 (1996).
- ⁸E. J. Hunter, I. R. Titze, and F. Alipour, "A three-dimensional model of vocal fold abduction/adduction," *J. Acoust. Soc. Am.* **115**(4), 1747–1759 (2004).
- ⁹J. Yin and Z. Zhang, "Interaction between the thyroarytenoid and lateral cricoarytenoid muscles in the control of vocal fold adduction and eigenfrequencies," *J. Biomech. Eng.-T. ASME* **136**(11), 111006 (2014).
- ¹⁰A. Gommel, C. Butenweg, K. Bolender, and A. Grunendahl, "A muscle controlled finite-element model of laryngeal abduction and adduction," *Comput. Methods Biomech. Biomed. Eng.* **10**(5), 377–388 (2007).
- ¹¹W. S. Selbie, S. L. Gewalt, and C. L. Ludlow, "Developing an anatomical model of the human laryngeal cartilages from magnetic resonance imaging," *J. Acoust. Soc. Am.* **112**(3), 1077–1090 (2002).
- ¹²E. J. Hunter and S. L. Thomson, "Solid CAD models of human laryngeal cartilage: Created from Selbie *et al.*, national repository for laryngeal data technical note," No. 6, April 2002, Version 1.0.
- ¹³Z. Zhang, "Characteristics of phonation onset in a two-layer vocal fold model," *J. Acoust. Soc. Am.* **125**(2), 1091–1102 (2009).
- ¹⁴B. A. Pickup and S. L. Thomson, "Influence of asymmetric stiffness on the structural and aerodynamic response of synthetic vocal fold models," *J. Biomech.* **42**(14), 2219–2225 (2009).
- ¹⁵H. E. Bateman and R. M. Mason, *Applied Anatomy and Physiology of the Speech and Hearing Mechanism* (Charles C. Thomas Publishers Ltd., Springfield, IL, 1984).
- ¹⁶K. Zhang, T. Siegmund, and R. W. Chan, "A two-layer composite model of the vocal fold lamina propria for fundamental frequency regulation," *J. Acoust. Soc. Am.* **122**(2), 1090–1101 (2007).
- ¹⁷Z. Zhang, J. Neubauer, and D. A. Berry, "Physical mechanisms of phonation onset: A linear stability analysis of an aeroelastic continuum model of phonation," *J. Acoust. Soc. Am.* **122**(4), 2279–2295 (2007).